

## Raman Study of Chromophore States in Photochromic Fluorescent Proteins

Stefano Luin,<sup>\*,†,‡</sup> Valerio Voliani,<sup>‡</sup> Giacomo Lanza,<sup>†</sup> Ranieri Bizzarri,<sup>†,‡</sup> Riccardo Nifosi,<sup>†,‡</sup> Pietro Amat,<sup>†,‡</sup> Valentina Tozzini,<sup>†,‡</sup> Michela Serresi,<sup>‡</sup> and Fabio Beltram<sup>†,‡</sup>

*NEST, Scuola Normale Superiore, CNR-INFM and Italian Institute of Technology, Piazza San Silvestro 12, 56124 Pisa, Italy*

Received June 13, 2008; E-mail: s.luin@sns.it

**Abstract:** The photophysical mechanism underlying the photochromic behavior of green fluorescent protein (GFP) mutants is investigated by means of preresonant Raman spectroscopy and model calculations. The studied molecules are reversibly switchable fluorophores that can be repeatedly converted between fluorescent and nonfluorescent states by irradiation and are attracting a broad interest for a number of new applications. Experimental results on chemically synthesized isolated chromophores are analyzed within a density functional theory approach that allows us to link the detected vibrational modes to specific ground-state configurations before and after photoconversion. These data are compared to results obtained for the case of complete folded proteins including the same chromophores. Our results highlight the impact of chromophore *cis*–*trans* isomerization and protonation state in the photophysics of these proteins and provide useful guidelines for novel mutant design.

### Introduction

Green fluorescent proteins (GFPs) truly revolutionized molecular and cellular biology. These fluorescent proteins (FPs) are the most widespread genetically encodable fluorescent markers and allow the direct, real-time monitoring of protein dynamics and interactions in living cells and tissues.<sup>1</sup> Specific mutations make it possible to tailor FP chemical and photophysical properties such as color, quantum yield, sensitivity to pH or other ions, and even their photochromic properties.<sup>2,3</sup> In particular, reversibly switchable fluorescent proteins (RSFPs) were developed that are capable of undergoing repeated transitions between states with different spectroscopic properties, e.g., fluorescent (*bright*) and nonfluorescent (*dark*) forms. This property makes RSFPs particularly attractive as *active* labels in biological systems for subdiffraction imaging or for selective photolabeling applications,<sup>4,5</sup> and they may even find use as single-molecule information storage devices.<sup>6</sup>

The photophysical basis for this peculiar behavior has yet to be fully understood and deserves attention, since it can help

guiding the detailed tailoring of mutant properties. In their pioneering work on the blinking and photoswitching behavior of a yellow mutant of GFP,<sup>7</sup> Dickson et al. suggested that the dark state they observed corresponded to a neutral form of the chromophore. In the case of a photoswitchable variant of cFP484 (mTFP0.7),<sup>8</sup> asFP595-A143S,<sup>9</sup> and Dronpa,<sup>10</sup> X-ray crystallographic studies showed that the brightness of these proteins is closely related to the conformation of the chromophore: the chromophore in the dark state is in a *trans* configuration, while in the bright state it shows a *cis* configuration. A similar mechanism was already proposed by some of us as a general feature of GFP-type RSFPs.<sup>11</sup> To date the test of this behavior was largely based on X-ray studies of protein crystals. This technique, however, is not applicable to proteins in solution or undergoing small conformational changes upon irradiation.<sup>12</sup> On the contrary, spectroscopic and in particular Raman studies of chromophores while embedded in folded proteins can provide detailed information on the chromophore structure, its interac-

<sup>†</sup> NEST, Scuola Normale Superiore and CNR-INFM.

<sup>‡</sup> NEST, Scuola Normale Superiore and Italian Institute of Technology.

- (1) Giepmans, B. N. G.; Adams, S. R.; Ellisman, M. H.; Tsien, R. Y. *Science* **2006**, *312*, 217–224.
- (2) Arosio, D.; Garau, G.; Ricci, F.; Marchetti, L.; Bizzarri, R.; Nifosi, R.; Beltram, F. *Biophys. J.* **2007**, *93*, 232–244.
- (3) Bizzarri, R.; Arcangeli, C.; Arosio, D.; Ricci, F.; Faraci, P.; Cardarelli, F.; Beltram, F. *Biophys. J.* **2006**, *90*, 3300–14. Bizzarri, R.; Serresi, M.; Luin, S.; Beltram, F. *Anal. Bioanal. Chem.*, published online Nov 26, 2008 <http://dx.doi.org/10.1007/s00216-008-2515-9>. Serresi, M.; Bizzarri, R.; Cardarelli, F.; Beltram, F. *Anal. Bioanal. Chem.*, published online Nov 27, 2008 <http://dx.doi.org/10.1007/s00216-008-2489-7>.
- (4) Stiel, A. C.; Trowitzsch, S.; Weber, G.; Andresen, M.; Eggeling, C.; Hell, S. W.; Jakobs, S.; Wahl, M. C. *Biochem. J.* **2007**, *402*, 35–42.
- (5) Lukyanov, K. A.; Chudakov, D. M.; Lukyanov, S.; Verkhusha, V. V. *Nat. Rev. Mol. Cell Biol.* **2005**, *6*, 885–890.

- (6) Cinelli, R. A. G.; Pellegrini, V.; Ferrari, A.; Faraci, P.; Nifosi, R.; Tyagi, M.; Giacca, M.; Beltram, F. *Appl. Phys. Lett.* **2001**, *79*, 3353–3355.
- (7) Dickson, R. M.; Cubitt, A. B.; Tsien, R. Y.; Moerner, W. E. *Nature* **1997**, *388*, 355–8.
- (8) Henderson, J. N.; Ai, H.-w.; Campbell, R. E.; Remington, S. J. *Proc. Natl. Acad. Sci. U.S.A.* **2007**, *104*, 6672–6677.
- (9) Andresen, M.; Wahl, M. C.; Stiel, A. C.; Grater, F.; Schafer, L. V.; Trowitzsch, S.; Weber, G.; Eggeling, C.; Grubmuller, H.; Hell, S. W.; Jakobs, S. *Proc. Natl. Acad. Sci. U.S.A.* **2005**, *102*, 13070–13074.
- (10) Andresen, M.; Stiel, A. C.; Trowitzsch, S.; Weber, G.; Eggeling, C.; Wahl, M. C.; Hell, S. W.; Jakobs, S. *Proc. Natl. Acad. Sci. U.S.A.* **2007**, *104*, 13005–13009.
- (11) Nifosi, R.; Ferrari, A.; Arcangeli, C.; Tozzini, V.; Pellegrini, V.; Beltram, F. *J. Phys. Chem. B* **2003**, *107*, 1679–1684.
- (12) Loos, D. C.; Habuchi, S.; Flors, C.; Hotta, J. i.; Wiedenmann, J.; Nienhaus, G. U.; Hofkens, J. *J. Am. Chem. Soc.* **2006**, *128*, 6270–6271.

tions with the environment, and in general the energy landscapes and the dynamics of the processes involved.<sup>13</sup>

Raman experiments on synthetic analogues of the GFP chromophore highlighted the differences in the vibrational spectra linked to the different protonation states.<sup>14</sup> The vibrational spectrum of the chromophore can be investigated also while inside fully folded proteins: preresonance conditions make it possible to selectively enhance the chromophore signal with negligible impact of the residual fluorescence. For example, this technique helped to determine the protonation of the chromophore before and after photoactivation in wild-type GFP (*wtGFP*).<sup>15</sup> Moreover, the differences of the Raman spectra in the two metastable states of a red RSFP brought up the question of a possible involvement of *cis*–*trans* isomerization in the photoswitching process.<sup>12</sup> To assess the possibility that *cis*–*trans* isomerization is a general feature of RSFPs, it is desirable to investigate systematically various chromophores, identify the fingerprints of their structural change, and then search these features in the Raman spectrum of the corresponding complete folded proteins.

To achieve this goal, we recently reported on the photochromic behavior of synthetic chromophores in their neutral forms.<sup>16</sup> Remarkably, we showed that they all undergo photoconversion when illuminated at the wavelength of maximum absorbance. The resulting photoproducts revert thermally very slowly (hours–days) or do not revert at all, if kept in organic aprotic solvents (like acetonitrile) at room temperature. On the contrary this photoconversion is fully reversible upon illumination at the appropriate wavelength. At least for the case of the analogue of the Y66F GFP (BFPF) chromophore, selectively decoupled <sup>13</sup>C-Nuclear Magnetic Resonance (<sup>13</sup>C NMR) spectra proved on a purely experimental basis that the native and photoconverted forms correspond to the *Z*- (*cis*) and *E*- (*trans*) stereoisomers, respectively. Combined NMR and absorption spectroscopy completed by accurate theoretical calculations showed that all the studied chromophores undergo the same *cis*–*trans* isomerization upon photoconversion.<sup>16</sup>

In this article we show for the first time the Raman spectra of both *cis* and *trans* forms of two of the chromophores, namely the analogues of (i) GFP and (ii) Y66F GFP (BFPF). Calculations based on density functional theory for preresonant Raman spectra are in full agreement with the experiments. Our investigation confirms *cis*–*trans* isomerization upon photoconversion. Based on this knowledge we analyze chromophore states when in the complete, folded protein in a blue and a yellow-green variant. Our approach allows us to identify the spectroscopic signatures of *cis*–*trans* isomerization and separate them from those linked to different protonation states of the chromophore.

## Materials and Methods

**Chromophore Synthesis.** The synthesis of model chromophores was accomplished by means of an established synthetic procedure involving two steps. First, the azalactone compounds were obtained through Erlenmeyer synthesis by reaction of *N*-acetylglycine,

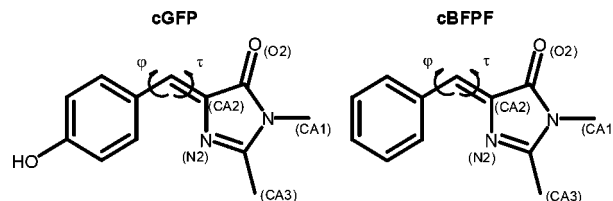


**Figure 1.** Molecular structures of cGFP [(*Z*)-4-(4-hydroxybenzylidene)-1,2-dimethyl-1*H*-imidazol-5(4*H*)-one] and cBFPF [(*Z*)-4-benzylidene-1,2-dimethyl-1*H*-imidazol-5(4*H*)-one]. In the figure are also labeled the angles  $\tau$  (involved in the “*cis*–*trans*” isomerization) and  $\varphi$  as well as the PDB nomenclature for the atoms cited in the text.

aromatic aldehydes, and anhydrous sodium acetate in acetic anhydride solution. In the second step, the aminolysis of the purified products with methylamine in the presence of sodium carbonate provided the corresponding chromophores. All details are reported in ref 16. Notably this procedure yields *Z*-isomers (*cis*) unless sterically hindered reactants are used in the first step,<sup>17,18</sup> which is not the case here. In the following, synthetic chromophores will be identified according to the corresponding protein name. Added prefixes will identify their stereoisomeric form (e.g., tGFP: *trans wtGFP* chromophore). In this work we investigate two different model chromophores: cBFPF (corresponding protein, BFPF) and cGFP (corresponding protein, *wtGFP*), which have respectively a phenyl and a 4-hydroxyphenyl substitute in the aromatic region (see Figure 1).

**Recombinant Fusion Proteins: Cloning, Expression, and Purification.** The ~2.9-kb vector pPR-IBA2 (IBA GmbH, Göttingen, Germany) was used for the expression of strep-tagged proteins. The cDNA of E<sup>3</sup>GFP was cloned into BsaI sites as described by Arosio et al.<sup>2</sup> To obtain the blue fluorescent protein (BFPF; main mutations from *wtGFP*: F64L Y66F), we performed a single-point mutation using the QuickChange Kit (Stratagene) according to the manufacturer’s instructions. The primers used to mutate the tyrosine (Y) in position 66 to phenylalanine (F) were purchased from Sigma-Genosys (St. Louis, MO). The sequence of sense primer used was CTCGTGACCACCCTGTCCTTCGGCGTGCAGTGCTTC. The antisense primer had the respective reverse complementary sequence. The green-yellow RSFP (EYQ1, main mutations from *wtGFP*: F64L T203Y E222Q) was obtained starting from E<sup>1</sup>GFP cloned in pPR-IBA2,<sup>2</sup> performing a single-point mutation to transform the residue 222 corresponding to a glutamic acid (E) into a glutamine (Q). The sense primer used was CACATGGTCTGCTGCAGTTCGTGACCGCCGCC. The antisense had the complementary reverse sequence. Expression of recombinant BFPF and EYQ1 proteins were induced in the log phase growing bacteria *E. coli* BL21 DE3 strain (Invitrogen) upon treatment with 1 mM isopropyl- $\beta$ -D-galactoside at 30 °C overnight. Proteins fused with a short peptide tag (MASWSHPQFEKGA) allowed purification by affinity chromatography with a strepTactin column (IBA BioTAGnology GmbH Göttingen) following manufacturer instructions. A further anion exchange purification step and concentration of the proteins were carried out using a Millipore Centricon Centrifugal Filter Unit by using a buffer with 50 mM diethanolamine (DEA) and 100 mM NaCl with the pH adjusted at 8.3 by adding HCl. The buffer could be exchanged with one at the desired pH by using the last method.

**Photoconversion Experiments and Absorption Spectroscopy.** Photoconversion experiments on chromophores were carried out by irradiating at 360, 406, and 458 nm using either an Ar–Kr laser (Beamlok 2060, Spectra Physics, Mountain View, CA, USA) or a Ti-sapphire IR-tunable laser (Mira 900, Coherent, Santa Clara, CA, USA) interfaced with a frequency doubler apparatus (SHG 9300, Coherent).

(13) Cinelli, R. A. G.; Tozzini, V.; Pellegrini, V.; Beltram, F.; Cerullo, G.; Zavelani-Rossi, M.; De Silvestri, S.; Tyagi, M.; Giacca, M. *Phys. Rev. Lett.* **2001**, *86*, 3439–3442.

(14) Bell, A. F.; He, X.; Wachter, R. M.; Tonge, P. J. *Biochemistry* **2000**, *39*, 4423–31.

(15) Bell, A. F.; Stoner-Ma, D.; Wachter, R. M.; Tonge, P. J. *J. Am. Chem. Soc.* **2003**, *125*, 6919–26.

(16) Voliani, V.; Bizzarri, R.; Nifosì, R.; Abbruzzetti, S.; Grandi, E.; Viappiani, C.; Beltram, F. *J. Phys. Chem. B* **2008**, *112*, 10714–10722.

(17) Mukerjee, A.; Kumar, P. *Heterocycles* **1981**, *16*, 1995–2034.

(18) Rao, Y.; Filler, R. *Synthesis* **1975**, *12*, 749–764.

The photoconversion of EYQ1 was obtained by irradiation at 514.5 nm using an argon laser (Stabilite 2017, Spectra-Physics). The photoconversion of BFPF was obtained by irradiation at 351 nm using the Ar–Kr laser or a Mercury lamp with a band-pass filter, obtaining a broad spectrum between  $\sim 360$  and  $\sim 375$  nm.

Typically, solutions of chromophores or proteins with an optical density from 0.5 to 0.8 were placed in 1500  $\mu\text{L}$  quartz cells with a 1 cm path length for absorption experiments; for the case of Raman and NMR experiments solutions with concentrations 1 to 10 mM were placed into 700  $\mu\text{L}$  quartz cells with a 0.5 cm path length or 20  $\mu\text{L}$  quartz cells with a 0.15 cm path length. All photoconversion experiments were performed at constant temperature by means of a Peltier thermostat (Varian, Palo Alto, CA, USA) and under continuous stirring. Ultraviolet–visible (UV–vis) spectra were measured on a Jasco 550 spectrophotometer (Jasco, Tokyo, Japan) with a Jasco ETC-505T thermostat.

**Raman Spectroscopy.** Preresonant Raman spectra of the chromophores were excited at 514.5 nm using the Argon laser. This wavelength was used to reduce the fluorescence signal and to avoid photoconversion during data acquisition. The inelastically scattered light was collected at an  $f$ -number of  $\sim 1$  through a Nikon objective or a 2'' convergent lens, filtered through a band-pass filter 525(50) (corresponding to an energy shift from the laser line in the range  $\sim 300$ – $1800$   $\text{cm}^{-1}$ ), and coupled with a bundle of optical fibers to an ACTON spectrometer Spectra Pro-300i equipped with 1200 g/mm gratings and with a nitrogen-cooled CCD for multichannel detection; the final resolution is  $\sim 5$   $\text{cm}^{-1}$ .

For each chromophore, we performed Raman measurements on solutions (1 to 10 mM) of the native *cis* isomer and its photogenerated mixtures containing both *cis* and *trans* isomers in  $\text{CH}_3\text{CN}$  and  $\text{CD}_3\text{CN}$ ; these solvents were chosen for the high solubility of the organic analytes and to minimize the impact of solvent Raman spectrum in the largest spectral range. Spectra were completed in up to 10 min using 150 mW laser power. The spectra of *cis* chromophores were obtained by subtracting the buffer spectra and signals due to elastically scattered light from the experimental spectra and then averaged with a weight related to the inverse of the solvent background. The spectra of *trans* chromophores were obtained by subtracting the *cis* chromophore spectra from those of the *cis/trans* photogenerated mixture and taking into account the mole fractions of each component as revealed by  $^1\text{H}$  NMR (and, in the case of c/tGFP, taking into account the thermal-decay rate).<sup>16</sup> The anionic cGFP chromophore was dissolved at 1 mM in an  $\text{H}_2\text{O}$  solution of NaOH at pH 9.9; this was brought to pH 6.3 by adding HCl to obtain the spectrum of neutral cGFP in aqueous solution as well. All the spectra were baseline-corrected to account for the background linked to residual fluorescence.

Protein Raman spectra were obtained with a similar setup, with excitation at 647 nm using the Ar–Kr laser, the collecting 2'' lens, and the filters of the Raman set Z647LP (Chroma Technology). The excitation wavelength was chosen to minimize fluorescence and to avoid photoconversion during data accumulation.

**Theoretical Calculations.** We performed optimization and vibrational-frequency analysis of the model chromophores using density functional theory (DFT), according to protocols some of us described in previous papers.<sup>19–21</sup> In particular, we used two different functionals (BLYP and B3LYP) and both the Plane Wave (PW) and Gaussian Bases (GB) implementations, whose chromophore-specific performance was described in detail by Nifosì et al.<sup>20</sup>

Preresonance Raman intensities were calculated by a numerical derivative of dynamic polarizability (through the Coupled Perturbed Hartree–Fock method), as implemented in the Gaussian 03 code<sup>22</sup>

using B3LYP and a 6–31G(d) basis of Gaussian wave functions (GB–B3LYP); we additionally evaluated the effect of the solvent within a polarized continuum model (PCM).<sup>23</sup> On-resonance Raman intensities were also evaluated within the PW–BLYP scheme with a simplified approach described by Tozzini and Giannozzi.<sup>24</sup> Although this approach does not exactly reproduce the experimental conditions, it is computationally advantageous and thus more appropriate to treat larger chromophores or to include some elements of the protein environment.

## Results

**Photochromism of the Chromophores.** Chromophore photochromism was already investigated by some of us in a previous article.<sup>16</sup> We wish to recall here that only one of the forms of BFPF and wrGFP chromophores was present in the native solutions. It was identified with cBFPF and cGFP ( $\tau = 0^\circ$  and  $\varphi = 0^\circ$ , see Figure 1), respectively. Following photoconversion a dramatic increase in tGFP and tBFPF molar fraction was observed.<sup>16</sup>

**Raman Spectra of the Two Isomers.** NMR data yield the structure of the BFPF chromophore (before and after photoconversion) on a purely experimental basis;<sup>16</sup> therefore we selected cBFPF as the benchmark for our preresonance Raman analysis. Figure 2a shows the Raman spectra of cBFPF and tBFPF. The latter is shown inverted with respect to the  $x$ -axis to allow a better comparison.

To confirm the structural conformation of the two isomers and to assign the measured spectral bands to specific vibrational modes, experimental spectra were compared to theoretical preresonance and on-resonance spectra calculated within the GB–B3LYP<sup>22</sup> and PW–BLYP<sup>24</sup> schemes, respectively. Preresonance calculations accurately reproduce sequence and relative intensity of the experimental peaks, except for a slight linear rescaling of the energy scale.<sup>25</sup> Figure 2b shows our calculated preresonance spectra in which a Lorentzian broadening (full width at half-maximum  $\nu/100$ , where  $\nu$  is the energy of the mode) was introduced to account for the experimental line broadening.<sup>26</sup>

Figure 3 shows the experimental Raman spectra of the dominant species before and after photoconversion for GFP in panel (a) and the calculated preresonance spectra for c/tGFP in panel (b), with the same conventions of Figure 2a,b. The spectrum of the anionic GFP chromophore in its native form (identified as a *cis* state) is reported as a dashed blue line in Figure 5; it is also shown in Figure S2, together with the spectrum of its photoconverted form in strongly basic conditions under continuous illumination at 404 nm.

**Identification of Signature Chromophore Vibrational Modes.** In the case of cGFP, our data are in general agreement with the Raman spectra previously discussed by other authors that assigned some of the vibrational modes.<sup>27,28</sup> By comparing *cis*

(19) Laino, T.; Nifosì, R.; Tozzini, V. *Chem. Phys.* **2004**, *298*, 17–28.

(20) Nifosì, R.; Amat, P.; Tozzini, V. *J. Comput. Chem.* **2007**, *28*, 2366–2377.

(21) Tozzini, V.; Bizzarri, A.; Pellegrini, V.; Nifosì, R.; Giannozzi, P.; Iuliano, A.; Cannistraro, S.; Beltram, F. *Chem. Phys.* **2003**, *287*, 33–42.

(22) Frisch, M. J.; et al. *Gaussian 03*, revision C.02; Gaussian, Inc.: Pittsburgh, PA, 2003.

(23) Cossi, M.; Barone, V. *J. Chem. Phys.* **2001**, *115*, 4708–4717.

(24) Tozzini, V.; Giannozzi, P. *ChemPhysChem* **2005**, *6*, 1786–8.

(25) The PW–BLYP scheme tends to underestimate and the B3LYP approach tends to overestimate the mode energy. See: Scott, A. P.; Radom, L. *J. Phys. Chem.* **1996**, *100*, 16502–16513.

(26) On-resonance calculations show a similar energy and intensity pattern for the modes with atom displacements analogous to the most intense modes in preresonant conditions, for both *cis* and *trans* configurations. However, some additional modes with a much higher calculated intensity are present, which are probably linked to modes that are Raman-active only under strictly resonant conditions; this perplexes the comparison with experiments.

(27) Esposito, A. P.; Schellenberg, P.; Parson, W. W.; Reid, P. J. *J. Mol. Struct.* **2001**, *569*, 25–41.

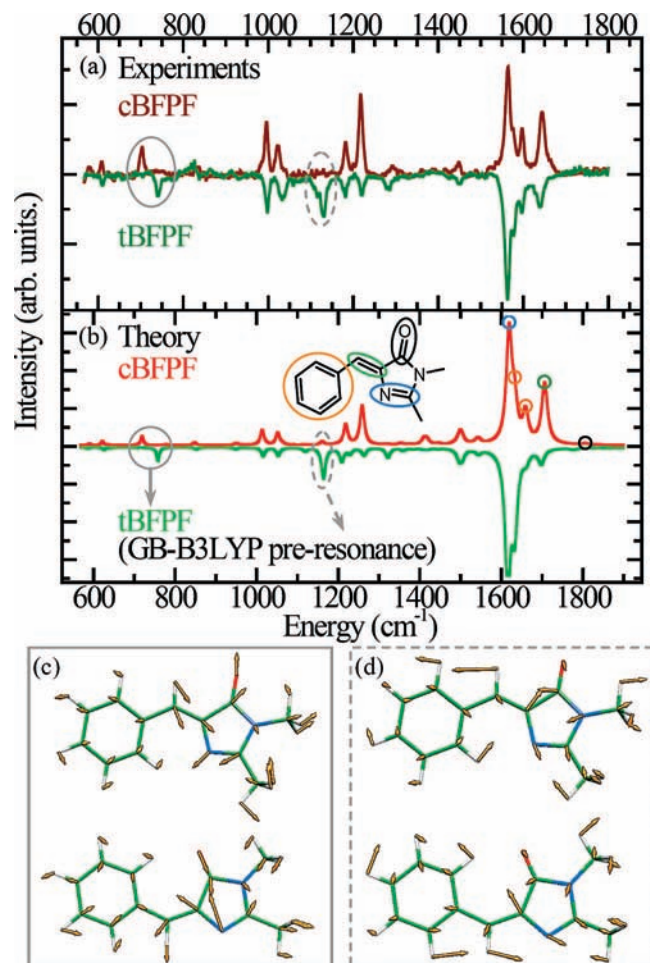


**Figure 2.** Experimental (a) and calculated *in vacuo* (b) preresonant Raman spectra of cBFPP and tBFPP; the spectra of the photoconverted form are shown inverted around the  $x$ -axis. Calculations are based on the B3LYP functional with Gaussian bases, considering an excitation at 514.5 nm. Solid and dashed gray ellipses highlight two of the modes that change significantly in the *cis*–*trans* transition and that are described in panels (c) and (d). Small circles emphasize stretching modes localized on double bonds in the chromophore region, highlighted in the inset of panel (b) with corresponding color: black, C=O; green, C=C on the bridge; orange, C=C on the phenylic ring; blue, C=N.

and *trans* spectra, one readily identifies three fingerprint regions common to all chromophore types that are present in both theoretical and experimental spectra.

First, we note that a band at around  $700\text{ cm}^{-1}$  undergoes a noticeable blue shift (about  $40\text{ cm}^{-1}$ ) upon isomerization (solid gray ellipses in Figures 2 and 3). Figure 2c shows that this band corresponds to a planar mode mainly localized on the bridge, on the heterocyclic ring, and on the methyl groups and that it involves a deformation of the N=C–C–C dihedral angle. These structural features are present in all the studied chromophores, and not surprisingly, a similar behavior (frequency location and blue shift) of this band is shared by all the structures.

Second, a group of bands at around  $1100\text{--}1300\text{ cm}^{-1}$  changes its intensity pattern upon *cis*–*trans* isomerization. The lowest-energy mode ( $\sim 1130\text{ cm}^{-1}$ ) undergoes a sharp intensity increase with cBFPP  $\rightarrow$  tBFPP and cGFP  $\rightarrow$  tGFP transitions (Figures 2 and 3, dashed gray ellipses). The theoretical analysis reveals

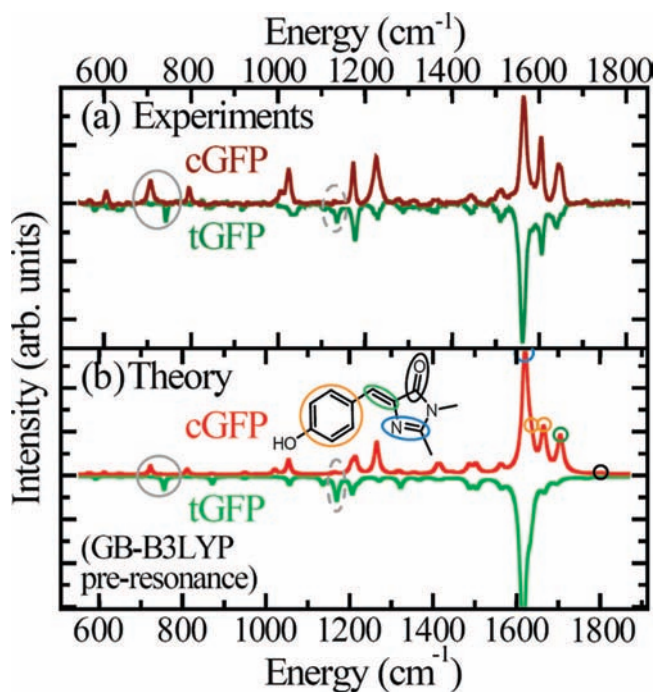


**Figure 3.** Experimental (a) and calculated *in vacuo* (b) preresonant Raman spectra of cGFP and tGFP; the spectrum of the *trans* form is shown inverted around the  $x$ -axis. Calculations are based on the B3LYP functional with Gaussian bases, considering an excitation at 514.5 nm. Solid and dashed gray ellipses highlight two of the modes that change significantly in the *cis*–*trans* transition, similar to those reported in Figure 2. Small circles emphasize stretching modes localized on double bonds in the chromophore region, highlighted in the inset of panel (b) with corresponding colors: black, C=O; green, C=C on the bridge; orange, C=C on the phenylic ring; blue, C=N.

that these bands are variously delocalized on the chromophore. The deformation pattern on the c/tBFPP for the lowest-energy mode is shown in Figure 2d; the higher intensity in tBFPP can be empirically linked to the higher impact of the stretching vibration of the NA2–CA2 chemical bond.

Finally, small but detectable shifts and intensity changes of the peaks in the  $1600\text{--}1720\text{ cm}^{-1}$  region are present. These are among the highest intensity modes and are attributable to vibrations localized on specific chromophore double bonds, as shown in the insets of Figures 2b and 3b.

Remarkably, similar features were found also in the Raman spectra of the two isomers of the analogue of the Y66W GFP chromophore<sup>16</sup> (c/tCFP, data not shown), confirming the general nature of the discussed Raman fingerprints.

**Photochromism of Complete Folded Proteins.** BFPP (F64L/Y66F GFP) is a blue fluorescent protein characterized by a rather weak emission ( $QY \approx 10^{-2}$ )<sup>29</sup> and absorption and fluorescence spectra quite close to those of the isolated chromophore.<sup>16</sup> Remarkably, we found that in BFPP all the phenomenology is quite similar to that of the isolated chromophore, apart from an increased photodegradation. BFPP in water at pH = 7 was laser irradiated at 360 nm for times up to 2 h and with power ranging from 5 to 100 mW. Significantly, upon continuous laser irradiation, the low-energy band decreased in intensity and was detectably red-shifted, and an isosbestic point at around 400 nm was observed (Figure S1a). We did not observe any thermal

(28) He, X.; Bell, A. F.; Tonge, P. J. *J. Phys. Chem. B* **2002**, *106*, 6056–6066.

(29) Kummer, A. D.; Kompa, C.; Lossau, H.; Pollinger-Dammer, F.; Michel-Beyerle, M. E.; Silva, C. M.; Bylina, E. J.; Coleman, W. J.; Yang, M. M.; Youvan, D. C. *Chem. Phys.* **1998**, *237*, 183–193.

recovery (Figure S1b). Irradiation at 405 or 458 nm of the photoconverted protein leads to an increase and blue shift of the low-energy absorption band and implies an at least partial recovery of the native state. More details on this protein absorption and photochromic behavior are provided in the Supporting Information.

EYQ1 is a yellow/green fluorescent protein, with spectral characteristics reminiscent of those of a similar mutant (T203Y E222Q *wf*GFP) studied by Jung et al.<sup>30,31</sup> We want to recall here that in this protein the chromophore is in equilibrium between two protonation states with  $pK = 6.86$  (see bottom of Figure 7); the protonated (form A) and anionic (form B) states are characterized by absorption and excitation spectra peaked at 410 and 511 nm, respectively.

The mutation E222Q inhibits the irreversibility of the photoactivation present in many GFPs, by removing the decarboxylation site on Glu222.<sup>31–33</sup> This simplifies the protein photophysics<sup>34</sup> and helps the analysis of Raman spectra. Long irradiation at 514 nm (30 min with power of 50 mW) of a 0.3 mM EYQ1 solution in water at pH = 8 led to a decrease of the fluorescence, a decrease of the absorption band peaked at 511 nm, and an increase of an absorption band at around 415 nm, similar to the one of the protonated chromophore. The thermal recovery of the native state is exponential with a lifetime of  $\sim 49$  min at this pH ( $\Delta$  arrow in Figure 7). Remarkably, the recovery time increases at lower pH and decreases at higher pH, being less than 50 s at pH  $\approx 10.4$ , where the protein begins to denature. A similar behavior was reported by Henderson et al. for mTFP0.7;<sup>8</sup> according to the authors, this fact could be linked to a possible protonation of the *trans* chromophore in the dark state.<sup>8</sup> While some speculations based on this observation will be discussed later, the details on the peculiar photophysics of EYQ1 as a function of pH are beyond the purpose of this paper and will be presented elsewhere.

**Raman Spectra of the Proteins.** Figure 4 shows the Raman spectrum of native BFPF excited by illumination at 647 nm (solid dark-red curves). All peaks detected in the chromophore at energies higher than  $900\text{ cm}^{-1}$  are also present in the protein spectrum, although some of them have a different intensity pattern or are slightly shifted. Additional peaks (highlighted by dotted black lines in Figure 4b) correspond to vibrational modes of the protein outside the chromophore region and arise in the spectrum because of the out-of-resonance condition. Indeed, the 647 nm excitation wavelength is relatively distant from the BFPF absorption peak (at  $\sim 360$  nm), and this hinders a highly selective enhancement of the chromophore modes against the background vibrations of other functional groups that are more represented within the protein matrix.

To obtain the Raman spectrum of the photoconverted protein, we shone light at a wavelength close to the absorption maximum while monitoring the absorbance and/or the fluorescence of the protein solution. This allowed us to monitor the achievement of a photostationary state. The spectrum of the photoconverted form was obtained from the experimental data after subtraction of the background and of the Raman signal originating from

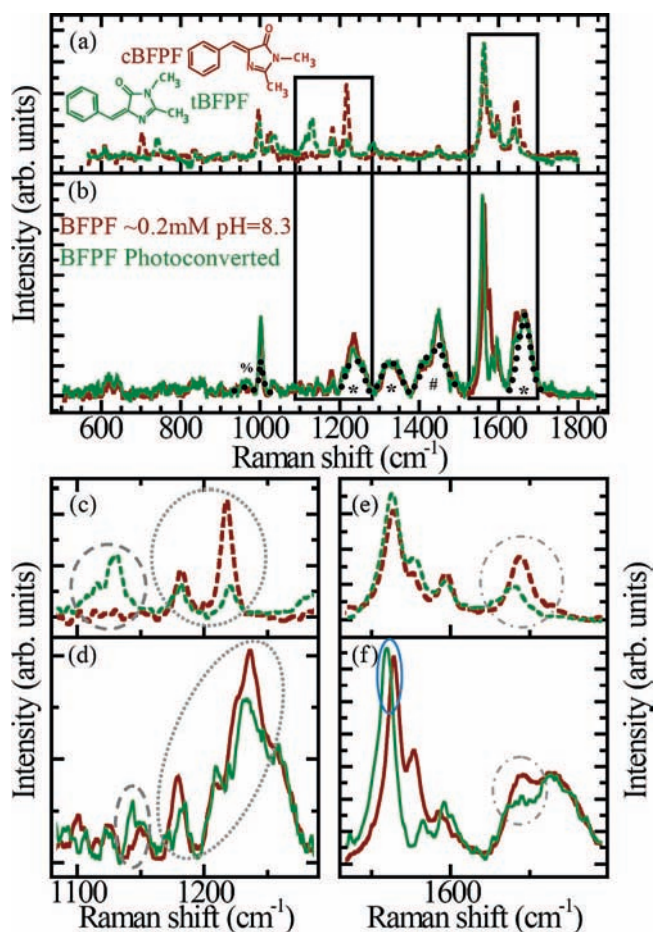


**Figure 4.** Solid curves: Raman spectrum of native BFPF (dark red) and of the photoconverted form only (dark green) after the subtraction of the baseline. The dotted black lines in panel (b) mimic the sharpest Raman peaks caused by the backbone of the protein and by the residues not entering in the chromophore (\*: amide modes; #:  $\text{CH}_2$ ,  $\text{CH}_3$  modes; %: phenylalanine modes, in particular the ring-mode at  $1004\text{ cm}^{-1}$  present in the chromophore as well). For comparison, dashed curves correspond to the Raman spectra of cBFPF and tBFPF (dark red and dark green dashed curves, respectively; same data of Figure 2a). The graphs in panels (c–f) are a magnification of the highlighted regions in panels (a) and (b); gray ellipses emphasize the main peaks changing in the same way in chromophore and protein going from native to photoconverted form. The blue ellipse in (f) emphasize a red shift of the  $\text{C}=\text{N}$  mode of the *trans* chromophore inside the protein.

the unconverted fraction. This spectrum is shown as solid dark-green curves in Figure 4. Notably, the peaks attributable to modes not related to the chromophore do not change, while the modification pattern of the chromophore modes is compatible with a *cis*–*trans* isomerization of the chromophore from the native to the photoconverted form of BFPF, as evident from the relative changes of the peaks highlighted by dotted and dashed gray ellipses and by the weakening and red-shift of the stretching mode of the  $\text{C}=\text{C}$  bridge (dash-dotted ellipses). The enhanced red shift of the  $\text{C}=\text{N}$  mode (blue ellipse in Figure 4f) is due to the details of the protein environment for the two isomers of the chromophore and will be discussed later.

We shall now discuss EYQ1 results. At pH = 8, its chromophore is mostly anionic. Therefore, in the top panel of Figure 5 we report the Raman spectrum of the anionic chemically synthesized chromophore in NaOH aqueous solution at pH = 9.9 (dashed blue line), compared with the spectrum of a neutral chromophore (dashed dark-green curve). The Raman spectrum of EYQ1 at pH = 8 is the blue curve in the bottom

(30) Jung, G.; Zumbusch, A. *Microsc. Res. Tech.* **2006**, *69*, 175–185.

(31) Jung, G.; Wiehler, J.; Zumbusch, A. *Biophys. J.* **2005**, *88*, 1932–47.

(32) van Thor, J. J.; Gensch, T.; Hellingwerf, K. J.; Johnson, L. N. *Nat. Struct. Biol.* **2002**, *9*, 37–41.

(33) Lippincott-Schwartz, J.; Altan-Bonnet, N.; Patterson, G. H. *Nat. Cell Biol.* **2003**, *Suppl.*, S7–14.

(34) Bizzarri, R.; Nifosi, R.; Abbruzzetti, S.; Rocchia, W.; Guidi, S.; Arosio, D.; Garau, G.; Campanini, B.; Grandi, E.; Ricci, F.; Viappiani, C.; Beltram, F. *Biochemistry* **2007**, *46*, 5494–5504.

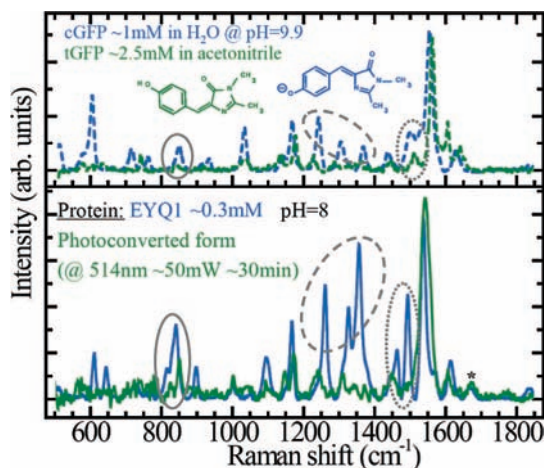


**Figure 5.** Bottom panel: Raman spectrum of native EYQ1 (blue solid line) and of the photoconverted form only (dark green solid line), at pH = 8, after the subtraction of the baseline. In the top panels are reported, for comparison, the Raman spectra of anionic cGFP (in aqueous solution of NaOH at pH = 9.9, dashed blue line) and of tGFP (in acetonitrile, same data of dark green curve in Figure 3a). Gray ellipses emphasize peaks discussed in the main text; \* indicates an amide I mode.

panel of Figure 5. The chromophore modes are now more intense than those in the previously discussed case. In this case, in fact, the excitation frequency is much closer to the chromophore resonance. Only one appreciable peak (at  $\sim 1670\text{ cm}^{-1}$ , labeled with \*) is present that probably is not linked to the chromophore and is caused by an amide I mode.

The Raman spectrum of the photoconverted form is plotted in the bottom panel of Figure 5 (solid dark-green curve). A comparison of the two spectra (Figure 5, bottom panel) strongly suggests that the photoconverted form contains a neutral chromophore. Note, e.g., the blue shift of the C=N peak at  $\sim 1540\text{ cm}^{-1}$  and the change in the intensity of the modes highlighted by ellipses in Figure 5 compared with the changes observed in the synthetic chromophore. This assignment for the protonation state of the photoconverted form is furthermore shown by the comparison of its Raman spectrum with the one of the native state of EYQ1 at low pH, discussed in the following paragraph. Finally, the Raman spectrum of the photoconverted synthetic chromophore of GFP in strongly basic conditions (see Supporting Information) is not compatible with the one of the photoconverted EYQ1 at pH = 8 (Figures S3 and S4).

To assign the stereoisomeric form of the chromophore in the photoconverted EYQ1, we compare its spectrum with the one of the same protein at pH = 4.7 (Figure 6, solid dark-red curves). The last spectrum is indeed very similar to the one of neutral cGFP (Figure 6, dashed dark-red curve), and the differences from the spectrum of the photoconverted form are small and consistent with the ones between neutral cGFP and tGFP; moreover, the comparison of Figure 6 with Figure 4 evidences the parallelism in the behavior of modes with similar atomic displacements in EYQ1 and BFPF compared with the case of their synthetic chromophores (like the enhanced red shift after photoconversion of the C=N mode or the weakening of the low-energy modes). This similarity with the case of BFPF, a protein where the chromophore does not have a protonation site on the phenyl ring, is further evidence that the chromophore of EYQ1 in the photoconverted form and the one in the native A form at low pH share the same protonation state and are therefore both neutral. We shall conclude that at pH  $\sim 8$  the native form of the protein contains an anionic *cis* chromophore,

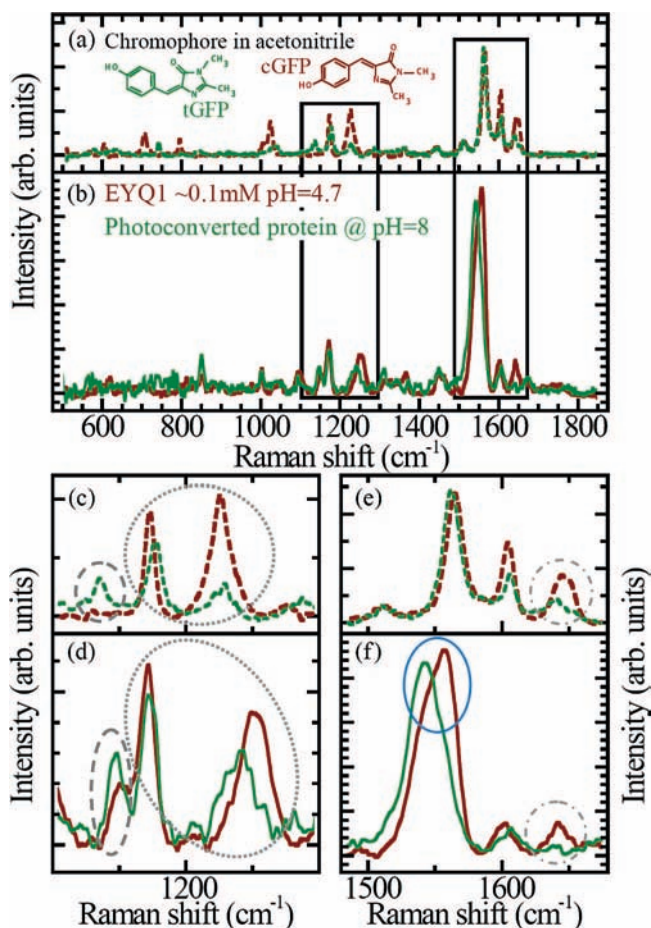


**Figure 6.** The dark red solid curves represent the Raman spectrum of native EYQ1 at pH = 4.7 after the subtraction of the baseline. For comparison are reported the Raman spectra of the photoconverted form at pH = 8 (dark green solid curve) and of neutral cGFP and tGFP (dark red and dark green dashed curves, same data of Figure 3a). Panels (c–f) are magnifications of the highlighted regions in panels (a) and (b); the ellipses emphasize peaks discussed in the main text.

while the photoconverted form contains a neutral *trans* chromophore.

## Discussion

The chromophore of FPs is a highly conjugated molecule encased by the external structure of the protein. In recent years, many experiments demonstrated that some GFP mutants present a complex photophysical behavior, which largely stems from the details of the chromophore molecular structure. One example is found in the (*Z*)-(E) diastereomerization of the chromophore, commonly called *cis*-*trans* isomerization. Under the assumption that this *cis*-*trans* isomerization represents a general feature of GFP chromophores, we synthesized the chromophore of two representative GFP mutants (Y66 and F66 GFP) and investigated the relation between their Raman spectral characteristics and their structural changes. In a previous article we showed that the chromophores can be reversibly photoconverted between *cis* and *trans* forms.<sup>16</sup>

**Fingerprints of Isomerization in Chromophores.** We report here the Raman spectra of the pure *trans* isomers, determined from the spectra of the photogenerated mixtures taking into account the mole fraction of each isomeric component. In all cases, experimental data were compared with theoretical calculations of the chromophore molecular structures and a

remarkable agreement between the two data sets was found. The most relevant fingerprints for the chromophores are highlighted in Figures 2 and 3. At lower energy, these are delocalized oscillations affecting also the bridge region involved in the *cis*–*trans* isomerization (various gray ellipses). At higher energy, there are some changes also for modes mostly localized on specific double bonds (colored circles), most evident for the mode localized on the bridge C=C.

The perfect agreement of the spectra of photoconverted forms with the corresponding calculated ones for *trans* isomers confirms that all the photoconverted chromophores do have a *trans* configuration, as demonstrated by some of us for the case of the chromophore of BFPF on a purely experimental basis and for the one of GFP by comparison with theoretical results.<sup>16</sup> We believe that the identification of the Raman fingerprints of *cis* and *trans* chromophore isomers is an important result that opens the way to analogous determination in the corresponding proteins.

**Isomerization in Photoconverted Proteins.** Raman spectroscopy is particularly suited for the determination of chromophore configurations within the protein fold, owing to its ability to selectively address the chromophore vibrational modes by means of resonant or preresonant excitation. We compared the Raman spectra of the chromophores with preresonant Raman spectra of BFPF and EYQ1. Experimental Raman spectra of proteins in their native form are dominated by *cis* chromophore modes; the presence of other peaks can easily be attributed to vibrations of structural groups in the rest of the protein. We were also able to determine the Raman spectra of photoconverted FPs (dark green solid curves in Figures 4, 5, and 6): they match the ones given by (neutral) *trans* chromophores.

Albeit small, some differences were observed in the spectra of the synthetic chromophores in solution (water or acetonitrile) with respect to those inside the proteins. These stem from two factors: the protein backbone (substituted in the chromophore by methyl groups centered on CA1 and CA3) and the different environment, i.e., a different network of hydrogen bonds, electrostatic interactions, and van der Waals interactions. The different environment is probably responsible for the red shift of the C=N stretching mode present in both photoconverted BFPF and EYQ1 (blue ellipses in Figures 4f and 6f), since in the *trans* form the N2 atom is more exposed to the protein environment, as shown for E<sup>2</sup>GFP by Nifosì et al.<sup>35</sup> Both factors cause the weakening of the lowest-energy detected modes (solid gray ellipses in Figures 2 and 3), not visible in the noisier low-energy part of the protein spectra, and of the modes highlighted by dotted and dashed gray ellipses in Figures 4 and 6; these changes were reproduced upon adding elements of the protein environment in on-resonant calculations, after the identification of the corresponding modes in preresonance calculations, but a detailed discussion of these issues goes beyond the scope of this paper.

With the confidence given by the aforementioned theoretical comprehension, our experiments demonstrate that the chromophore of the photoconverted form of the analyzed GFP variants has a *trans* configuration. We are also able to prove, on an experimental basis, the neutrality of the EYQ1 chromophore in the photoconverted *trans* form. The *trans* chromophore can be protonated at a pH where the *cis* isomer is anionic because of the different, more hydrophobic cavity environment in the protein for the phenolic ring within the *trans*

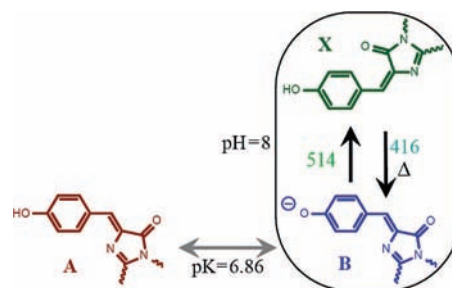


**Figure 7.** Proposed scheme for the considered states of the chromophore in EYQ1. A and B follow the usual nomenclature for proteins of the GFP family; X is the proposed predominant photoconverted form at pH = 8. Undulated lines indicate the link with the protein backbone. The numbers indicate the wavelengths used for the photoconversions;  $\Delta$  indicates a thermal decay.

chromophore, as was suggested by molecular dynamics studies for the case of E<sup>2</sup>GFP,<sup>35</sup> or for homologous fluorescent proteins from other sea organisms on account of crystallographic studies.<sup>8,10</sup> In particular, Andresen et al.<sup>10</sup> highlighted the different electrostatic surface potentials and the weaker hydrogen bonds and van der Waals force network around the *trans* chromophore in the fluorescent protein *Dronpa*.

This reduced H-bond coordination between the *trans* chromophore and the protein matrix probably increases the torsional freedom of the chromophore, inducing a more efficient nonradiative decay from its excited state and, therefore, a loss of fluorescence intensity.<sup>35</sup> When the *trans* chromophore is protonated, the blue shift of the excitation peak will contribute to reduce the excitation of form A excited close to the maximum for form B, therefore the observed fluorescence; in the same case, also a hindered excited-state proton transfer (ESPT) was mentioned as partially responsible for the darkness of the state.<sup>35</sup>

The different acid–base equilibrium in the photoconverted state is probably responsible also for the previously cited pH dependence of the thermal stability of the photoconverted form in EYQ1 (see also ref 8). Indeed, the observed phenomenology may be explained by a higher overall stability of the neutral form in the *trans* state compared to its anionic counterpart, owing to the protein environment; this was also suggested by theoretical calculations.<sup>36</sup> From this perspective, raising the pH leads to an increase in the population of the *trans* anionic form and correspondingly to a faster decay back to the *cis* state. Nonetheless, more experiments are needed to fully dissect the subtle interaction between the thermally and optically driven photoswitching of RSFPs in different environments to address, e.g., its influence of blinking and flickering phenomena seen in single molecule spectroscopy or to develop mutants with more stable dark states.

## Conclusions

We have presented a detailed study of the Raman signatures of different chromophore states in GFP-derived fluorescent proteins and compared these to the ones relative to isolated chemically synthesized chromophores. Our investigation allowed us to demonstrate on a purely experimental basis that the *cis*–*trans* isomerization (*Z*–*E* diastereomerization) of the chromophore is responsible for the photochromic properties of at least two of these proteins.

The Raman spectra of the *trans* forms (*E*-isomers) of BFPF- and GFP-like protein chromophores were shown and compared to the ones of the (native) *cis* forms (*Z*-isomers). Experimental results were analyzed within a time-dependent density functional

(35) Nifosì, R.; Tozzini, V. *Chem. Phys.* **2006**, *323*, 358–368.

theory. The good agreement between calculated and experimental spectra allowed us to assign all relevant experimentally observed modes in both *cis* and *trans* isomers in the spectral region between 600 and 1800  $\text{cm}^{-1}$ . These data have been compared to results obtained for the case of complete folded proteins in two cases. For the BFPP we showed that the chromophore is in a *cis* configuration in the native form, while it is *trans* in the photoconverted form. For the case of EYQ1 we showed that at  $\text{pH} = 8$  the chromophore is anionic in the native form and neutral *trans* in the photoconverted form; it is neutral *cis* in the native form at lower pH. The last results are summarized in Figure 7.

Our investigation highlights the relevance of Raman spectroscopy for the study of ground and metastable states of

optically active portions of proteins in solution, since Raman is a nondestructive technique that allows one to monitor on-the-flow the products of photoconversion. Finally, our results support the hypothesis that *cis-trans* isomerization is a general feature in RSFPs.

**Acknowledgment.** This research was supported in part by the Italian Ministry for University and Research under FIRB No. RBLA03ER38 and by the Fondazione Monte dei Paschi di Siena.

**Supporting Information Available:** Details of the photophysics of BFPP, with one figure. Photoconversion of cGFP in strongly basic conditions, with three figures. Complete ref 22. This material is available free of charge via the Internet at <http://pubs.acs.org>.

JA804504B

(36) Weber, W.; Helms, V.; McCammon, J. A.; Langhoff, P. W. *Proc. Natl. Acad. Sci. U.S.A.* **1999**, *96*, 6177–82.